Potential Heterogeneous Catalysts from Three Biogenic Residues toward Sustainable Biodiesel Production: Synthesis and Characterization

Christopher Tunji Oloyede,[a] Simeon Olatayo Jekayinfa,*[a] Abass Olanrewaju Alade,[b] Oyetola Ogunkunle,[c] Opeyeolu Timothy Laseinde,[c] Ademola Oyejide Adebayo,[a] Ibham Veza,[d] and Islam Md. Rizwanul Fattah*[e]

The cost and difficulty in the preparation of synthetic heterogeneous base catalysts is the main barrier to their use. Today, the majority of these catalysts are derived from biomass resources. This study aimed at developing and characterizing these catalysts from three biogenic residues for biodiesel production without catalyst support. The EDS indicated the variation of Na, K, Mg, and Ca, having aggregates of 67.45, 83.15, and 76.85% in calcined- periwinkle shell-ash (CPWSA), -melon seed-husk ash (CMSHA) and -locust bean pod ash (CLBPA), respectively. XRD revealed the presence of sodium oxide (Na_2O), calcium oxide (CaO), potassium oxide (K_2O), and magnesium oxide (MgO) in the catalysts at 800°C. The FTIR showed the presence of C=O, C−H, and O−H bonds in the catalyst samples. The basicity values of CPWSA, CMSHA, and CLBPA are 11.65, 10.41, and 11.62, respectively. The developed catalysts were used to synthesize biodiesel from palm kernel oil.

Introduction

The global community is currently searching for an alternative, renewable and eco-friendly energy sources due to the gradual depletion and environmental pollution of fossil fuels that release obnoxious and poisonous emissions into the atmosphere.[1] Biodiesel, being one of the most probable alternative biofuels, is of increasing research and commercial interest because its renewable, non-toxic and environmentally friendly.[2] However, its cost of production depends majorly on the feedstock used, which is a crucial challenge to its full global acceptance.[3] Biodiesel is majorly produced via a transesterification reaction between vegetable oil or animal fats and alcohol in the presence of a catalyst that could either be homogeneous or heterogeneous.[4] The commonly used catalyst for this reaction to synthesize biodiesel is a homogeneous catalyst such as sodium hydroxide (NaOH) or potassium hydroxide (KOH) because it gives better activity and yield in a short time.[5] Different researchers have worked on biodiesel production using homogeneous catalysts.[6] Still, the major disadvantages of using homogeneous catalysts for biodiesel synthesis include difficulty in product separation, soap formation and catalyst recovery. In the search for an alternative catalyst as a replacement for homogeneous catalysts, the research community found that heterogeneous catalysts have abilities to overcome the associated difficulties with homogeneous catalysts; because they are renewable, reusable, eco-friendly and easily separated from the reaction mixture.[7] Heterogeneous catalysts could be base, acid, or enzymatic in nature. Calcium oxide (CaO) and $CaO-MoO_3$ are two examples of heterogeneous base catalysts.[8] Among the heterogeneous solid-acid and enzymatic catalysts are aluminium hydrogen sulphate $Al(HSO_4)_3$ and lipase.[9] Nonetheless, the cost of these heterogeneous catalysts is the main barrier to their use, as the majority of them are expensive and difficult to prepare on a large scale, limiting their potential use in industrial operations.[10]

The majority of heterogeneous catalysts today are derived from biomass resources such as plants and animals. Because biomass sources are abundant, cheaper, renewable, and sustainable, they are preferred in developing heterogeneous catalysts.[3,11] These catalysts are frequently derived from natural biological sources that are rich in calcium (Ca) or potassium (K) compounds. The oxide of these elements has the potential to

[a] C. Tunji Oloyede, S. Olatayo Jekayinfa, A. Oyejide Adebayo
Department of Agricultural Engineering, Ladoke Akintola University of Technology, Nigeria
E-mail: sojekayinfa@lautech.edu.ng
Homepage: http://age.lautech.edu.ng/engr-prof-s-o-jekayinfa-2

[b] A. Olanrewaju Alade
Department of Chemical Engineering, Ladoke Akintola University of Technology, Nigeria

[c] O. Ogunkunle, O. Timothy Laseinde
Department of Mechanical and Industrial Engineering Technology, University of Johannesburg, South Africa

[d] I. Veza
Department of Mechanical Engineering, Universiti Teknologi PETRONAS, 32610 Bandar Seri Iskandar, Perak Darul Ridzuan, Malaysia

[e] I. M. Rizwanul Fattah
Centre for Technology in Water and Wastewater (CTWW), School of Civil and Environmental Engineering, Faculty of Engineering and IT, University of Technology Sydney, Ultimo, 2007, NSW, Australia
E-mail: IslamMdRizwanul.Fattah@uts.edu.au
Homepage: https://profiles.uts.edu.au/IslamMdRizwanul.Fattah

ChemistrySelect

Research Article
doi.org/10.1002/slct.202203816

**Chemistry
Europe**
European Chemical
Societies Publishing

be heterogeneous base catalysts for the transesterification of triglyceride.[12] The production of heterogeneous catalysts entails a series of simple methods with low energy requirements.

More than 700,000 tons of agricultural crop residues generated in Nigeria contribute to environmental pollution, but these residues have diverse areas of potential applications in energy generation.[13] Agricultural residue-derived calcined ashes have been widely studied as heterogeneous base catalysts in biodiesel production.[14] Previous reports have demonstrated the use of different agricultural residues in developing heterogeneous base catalysts. The basis is to discover abundant plant or animal biomass residues of high catalytic properties which can be efficiently used sustainably. Heterogeneous base catalysts have been produced from calcined- rubber seed shell,[15] ostrich-eggshell,[16] snail shell,[6b] banana peels,[17] ripe plantain peels,[18] *Brassica nigra* plant,[19] capzi shell,[10] moringa leaf,[20] duck eggshell,[13c] ripe and unripe plantain peels mixture,[12] among others for triglycerides transesterification.

Due to the abundant nature of periwinkle shell residues (38.5 tons) which are naturally rich in calcium carbonate,[21] melon seed husk (about 500,000 tons/y), which is rich in Ca, K, and Na[22] and locust bean pod husk (about 200,00 tons/y) which is rich Ca, K and magnesium compounds[23] making them be further studied as a suitable feedstock for the development of heterogeneous base catalysts. There seems to be limited information on the development of heterogeneous base catalysts from these biogenic residues for biodiesel synthesis despite the fact that they are rich in alkali elements whose oxide is suitable to be used as a heterogeneous base catalyst. So, the novelty of this study is the utilization of calcined periwinkle shells, locust bean pod husk and melon seed husk as sources of Ca, K, Na or Mg oxides or compounds as heterogeneous base catalysts for biodiesel production without catalyst support.

Experimental Section

The agricultural residues used for the research and the methodology for catalyst preparation are reported in detail in this section.

Materials

The agricultural residues, melon, and locust bean husks used in this study were collected from Aroje (8°19′N 4°26′E), Ogbomoso, Nigeria. Periwinkle shells were sourced from Igbokoda (6°21′N 4°47′E), Nigeria. The biogenic materials were obtained from these locations because of their availability in high proportions.

Sample preparation

The selected residues were washed at least three times with tap water, followed by distilled water to remove dissimilar materials, and then dried under solar irradiation for three days. The sundried residues were oven dried at 100 °C to a constant weight to reduce their moisture content. The oven-dried residue was ground separately into powder using a disk mill and sieved to a particle

size of 150 μm using a standard sieve via a mechanical shaker. Each sieved sample was kept in airtight containers for further analysis. Sample preparation follows the method reported by Betiku et al.[17] and Mendonça et al..[24]

Catalyst synthesis

A portion of each of the periwinkle shell, melon seed husk and locust bean pod-husk powder samples were kept as raw samples. Another portion each was calcined at varying temperatures (600, 700 and 800 °C respectively) for 4 hours in a muffle furnace (Galenkamp) to obtain fine ash and to remove carbonaceous and volatile matter from them.[25] The calcined ash samples (the catalyst) from each selected residue were put in Ziplock bags before being stored in airtight containers and then kept in a desiccator for further studies and to avoid reaction with carbon (IV) oxide and relative humidity. Each calcined ash sample from each residue was designated as calcined periwinkle shell ash (CPWSA), calcined melon seed husk ash (CMSHA) and calcined locust bean pod-husk ash (CLBPA) catalysts. The catalyst preparation followed procedures detailed by Mendonça et al.[24] and Okoye et al..[21b]

Catalyst characterization

The catalysts (CPWSA, CMSHA, and CLBPA) were characterized to learn more about their properties. The elemental compositions of each catalyst were determined using an Energy Dispersive X-ray spectrometer (JEOL JSM-7600F, Japan), and the diffractograms obtained were recorded with a Gatan alto 2500 Cryo system. Fourier Transform Infrared (FTIR) examination utilizing a Thermo Nicolet iS10 FTIR spectrometer (Thermo Fisher, Madison, USA) was used to determine the functional groups on the active site of the catalyst's surface. The resulting spectra were obtained in the 4000 to 400 cm^{-1} range. The crystalline phases in CPWSA, CMSHA, and CLBPA were determined using an X-ray diffractometer via Rigaku-binary (Chicago, USA). The sample analysis involves a continuous scan of the sample in locked coupled mode with Cu–Kα_2 radiation at a wavelength of 1.5444 Å, 45 kV voltage, and 40 mA current. The samples were scanned at a speed of 5°/min in the 2θ range of 5–76°. The catalyst characterization follows the procedure reported by Aladetuyi et al.,[26] Falowo et al.,[27] and Etim et al..[28]

Catalytic testing of the developed heterogeneous catalysts

The strength of the developed CPWSA, CMSHA and CLBPA biobased catalysts was tested via transesterification of palm kernel oil (PKO). The transesterification of PKO was conducted in a three-necked round bottom flask of 500 ml equipped with a reflux condenser, heating source controller, thermometer, and magnetic stirrer.[29] The transesterification procedure was carried out under the reaction condition with an ethanol-to-oil ratio at 6:1, catalyst loading at 7.0 wt.%, reaction temperature at 65 °C and reaction time at 120 minutes at a constant agitation of 700 rpm until the completion of the reaction. At the end of the reaction, the catalyst was recovered through filtration using Wartman filter paper (100 microns). The mixture was then poured into a separating funnel and allowed to separate into two distinct layers, with the top layer being the biodiesel, also known as Palm Kernel Oil Ethyl Ester (PKOEE), and the lower layer being a mixture of excess ethanol and glycerol. After separation, the excess ethanol was removed by evaporation at a temperature of 78 °C. The quantity of the biodiesel obtained was measured using equation 1.

ChemistrySelect

Research Article
doi.org/10.1002/slct.202203816

Chemistry Europe
European Chemical
Societies Publishing

$$B_y \ (\%) = \frac{W_b}{W_o} \times 100 \qquad (1)$$

Where: B_y = biodiesel yield, W_b = weight of biodiesel produced and W_o = weight of oil used.

Determination of fuel properties and fatty acid composition of PKOEE

The fuel properties of the PKOEE samples obtained using CPWSA, CMSHA and CLBPA catalysts were characterized to determine their qualities. The kinematic viscosity and specific gravity were determined using a Cannon-Fenske Capillary Viscometer tube (CFRC-100) and pycnometer following the procedure in ASTM D445-19a and ASTM D1298, respectively. The flash point of the biodiesel samples was determined according to ASTM D-93 using an automated Penske-Martens closed cup apparatus (PMA 5, Ducom Instrument Company, USA), while the cloud and pour point were analyzed using ASTM D2500 and ASTM D97, respectively. The iodine cetane number and calorific value were determined using AOAC 2012 method and according to Oladipo and Betiku.[2a] Using equations 2 and 3, respectively.

$$C_n = 46.3 + \frac{5458}{SV} - (0.225 x IV) \qquad (2)$$

$$C_v = [(0.041 x SV) + (0.05 x IV)] \qquad (3)$$

Where: C_n and C_v are the cetane number and calorific value, respectively, SV is the saponification value, and IV is the iodine value. The fatty acid methyl esters composition of PKOEE produced was analyzed as described by Odude et al.[30] using a Gas Chromatography (910-GC, 6-detector system, Buck Scientific, SRI Instruments, USA) with a power rating of 230VAC±10% 1725 W, and using helium gas as carrier gas.

Results and Discussion

EDX results of CPWSA, CMSHA and CLBPA at varying temperature

One of the essential factors that control the behaviour of a bio-based catalyst is the kind of elements present in such a catalyst.[28] The EDX analysis was used to recognize the elements present in the raw powder samples from the periwinkle shell, melon seed husk, locust bean pod and their calcined ash samples obtained by calcination of the powdered samples at varying temperatures of 600, 700, 800 °C. The results showed that the CPWSA, CMSHA and CLBPA contained elements such as Na, K, Al, Mg, Ca, Mn, Si, P and Fe (Table 1). It was observed that for CPWSA, CMSHA and CLBPA catalysts, calcium (Ca) has the highest mass fraction irrespective of the calcination temperature. Calcium has the highest mass fraction in CPWSA and CMSHA catalyst at 700 °C with 61.11 and 66.73%, respectively, but 70.74% in CLBPA catalyst at 800 °C. Etim et al.[18] and Olatundun et al.[31] reported similar elemental constituents for calcined ripped plantain peels ash (CRPPA) and calcined blended cocoa pod and plantain peels ash. It has been reported that the presence of alkali and alkaline earth metals such as K, Na, Ca, or Mg favours the use of calcined ash samples derived from agricultural residues as biobased heterogeneous catalysts in the transesterification of oil into biodiesel.[24] Hence, the mass fraction of the alkali and alkaline earth metals present was considered by taking the sum of the mass fraction of each of these metallic elements present in each of the CPWSA, CMSHA and CLBPA catalysts at different calcination temperatures.

As revealed in Table 2, the total mass fraction of alkali and alkaline earth metals in CPWSA and CMSHA catalysts were 67.45% and 83.15%, respectively, at a calcination temperature of 700 °C, and 76.85% for CLBPA at 800 °C. The fluctuating variability of the total percentage of alkali and alkaline earth metals could be attributed to the density and thermal stability ability of these metals as present in the calcined ash sample at each varying temperatures.[32] The higher concentration of these elements in CPWSA, CMSHA and CLBPA could contribute an excellent catalytic behaviour, thus, making them potential heterogeneous base catalysts in the transesterification of oils into biodiesel. Mendonça[24] reported a high percentage of alkali and alkaline earth metals (K, Ca and Mg) of 88.0% in calcined *tucumã* peels ash catalyst (CTPAC) at a temperature of 800 °C, which favours the use of the material as a heterogeneous base catalyst.

Table 1. Elemental composition of CPWSA, CMSHA and CLBPA catalysts at different temperatures.												
Catalyst	Calcination temp. [°C]	Elemental composition in each catalyst [wt.%]										
		Na	K	Al	Mg	C	Ca	O	Fe	Si	P	Mn
CPWSA												
	600	2.20	0.00	10.30	1.32	3.20	58.72	12.20	7.34	0.10	4.25	0.00
	700	0.72	3.75	10.33	1.87	5.22	61.11	11.74	4.62	0.59	0.00	0.00
	800	2.20	0.10	10.40	0.35	4.20	60.60	15.30	3.52	3.33	0.00	0.00
CMSHA												
	600	1.06	1.12	5.10	4.52	3.85	65.23	10.83	3.92	3.68	0.69	0.00
	700	0.80	12.80	2.30	2.82	3.17	66.73	15.99	3.55	0.26	0.58	0.00
	800	0.78	12.68	2.45	2.99	5.18	55.98	10.68	3.58	0.17	5.51	0.00
CLBPA												
	600	2.24	0.00	2.76	0.33	7.24	60.72	19.52	6.55	0.86	0.00	0.00
	700	0.20	10.00	3.40	3.36	9.00	54.70	14.60	2.60	1.40	0.00	1.10
	800	0.82	0.84	1.53	4.45	5.29	70.74	10.43	3.14	2.31	0.00	5.51

ChemistrySelect

Research Article
doi.org/10.1002/slct.202203816

Chemistry
Europe
European Chemical
Societies Publishing

Table 2. Elemental compositions of alkaline elements in CPWSA, CMSHA and CLBPA.

Sample	Calcination temp [°C]	Alkali and alkaline earth metals in each calcined ash sample [wt.%]				
		Na	K	Mg	Ca	Total
CPWSAC						
	600	2.2	0	1.32	58.72	62.24
	700	0.72	3.75	1.87	61.11	67.45
	800	2.2	0.1	0.35	60.6	63.95
CMSHAC						
	600	1.06	1.12	4.52	65.23	71.93
	700	0.8	12.8	2.82	66.73	83.15
	800	0.78	12.68	2.99	55.98	72.43
CLBPAC						
	600	2.24	0	0.33	60.72	63.29
	700	0.2	10	3.36	54.7	68.26
	800	0.82	0.84	4.45	70.74	76.85

Figure 1 showed the spectral of the EDX analysis contained a mass fraction of elemental compositions for both the uncalcined (raw) and the calcined ash samples of periwinkle shell, melon husk and locust bean pod-husk, for the appreciable calcination temperature that showed the highest mass fraction for calcium (Ca). The differences in elemental mass fraction, combined with the fact that certain elements present in the uncalcined samples were absent in the calcined ash samples, demonstrate that calcination temperature influences the elemental composition of each sample. This is attributed to the effect of temperature during the thermal decomposition of the raw samples at higher temperatures.[28]

XRD results of CPWSA catalyst at varying temperatures

The XRD patterns of uncalcined periwinkle shell powder, UPWSP and CPWSA were investigated at different calcination temperatures of 600, 700 and 800 °C. This is to clarify their potential crystalline structure's contribution to catalytic performance and identify the crystalline phases present in the raw and calcined ash samples. It was observed from Figure 2 that the XRD pattern of UPWSP consists mainly of the orthorhombic crystalline phase of aragonite ($CaCO_3$) with lattice parameters $a = 4.959$ Å, $b = 7.968$ Å and $c = 5.741$ Å as indicated by the major diffraction peaks at 2θ of $26.28°$, $33.11°$, $37.89°$, $45.92°$, $48.37°$ and $52.49°$ with JCPDS reference code 00-005-0453. According to Shanahan et al.[33] and Boonyuen et al.,[34] aragonite is formed because of precipitation from marine and freshwater environments, and molluscs need to form their shells. Then, the presence of the crystalline phase of aragonite in the raw sample of dried periwinkle shell powder at a reference temperature of 100 °C may be a result of the precipitation of aragonite in their aquatic habitat. Aragonite has been reported for an uncalcined sample of *Turbo jordani* shells by Boonyuen et al..[34]

The CPWSA catalyst at 600 and 700 °C showed primarily the rhombohedral crystalline phase of calcite or calcium carbonate ($CaCO_3$) with lattice parameters $a = b = 4.988$ Å and $c = 17.053$ Å (JCPDS reference code 96-900-0227; 01-083-0578, respectively). Wray and Daniels[35] de-tailed that calcium carbonate takes two mineral forms, which are calcite and aragonite, but a higher temperature above 400 °C favors the conversion of aragonite into calcite. Therefore, this revealed that at calcination temperatures of 600 and 700 °C, respectively, aragonite in the raw sample was converted to calcite ($CaCO_3$). Therefore, the diffraction peaks of calcite were shown at 2θ of $26.22°$, $27.21°$, $33.13°$, $39.43°$ and $65.62°$ for calcination temperature of 600 °C and at 2θ of $23.07°$, $29.43°$, $39.43°$, $47.53°$ and $57.42°$ for calcination temperature of 700 °C. Also, the crystalline phase of anorthite, $CaAl_2(SiO_4)_2$, (JCPDS reference code 00-002-0523), which is also one of the mineral forms of carbonate, was found at $2\theta = 49.12°$ and $49.12°$. Ekeoma et al.[36] also identified this mineral in clay formulation catalyst for biodiesel production. Therefore, the formation of anorthite at this peak might be due to the precipitation of clay material during periwinkle shell formation. Moreover, the CPWSA at 800 °C showed the peaks of the cubic crystalline phase of calcium oxide (CaO) with lattice parameters $a = b = c = 4.802$ Å at 2θ of $29.54°$, $32.29°$, $37.52°$, $48.60°$, $50.92°$ and $53.94°$ (JCPDS reference code 01-077-2010).

The formation of CaO in CPWSA catalyst at 800 °C might be due to the thermal decomposition of calcite ($CaCO_3$) at a higher temperature. However, there are still phases of calcite at this temperature which shows that complete thermal decomposition of the shell requires a higher temperature above 800 °C. Suryaputra et al.[10] detailed similar results for the formation of calcium oxide from calcined capiz shell at 900 °C, which contained calcite in its natural form. Furthermore, the monoclinic crystalline phase of calcium iron oxide, $Ca_2Fe_7O_{11}$ (JCPDS 01-083-1903; $a = 9.960$ Å, $b = 3.030$ Å and $c = 15.77$ Å), hexagonal crystalline phase of sodium oxide, Na_2O (JCPDS 01–074-0111; $a = b = 6.208$ Å and $c = 4.802$ Å) and rhombohedral crystalline phase of calcite were present in CPWSA catalyst at 800 °C. The diffraction peaks for $Ca_2Fe_7O_{11}$, Na_2O and $CaCO_3$ were shown at 2θ of $17.80°$, $34.21° and$ $39.49°$ for $Ca_2Fe_7O_{11}$; $29.51°$, $47.61°$ $57.45°$ and $65.67°$ for Na_2O and $29.51°$, $43.22°$ and $65.67°$ for $CaCO_3$, respectively. Due to the presence of metallic oxide of alkaline metals and mixed metal oxide, which have good catalytic behaviour for biodiesel production at a
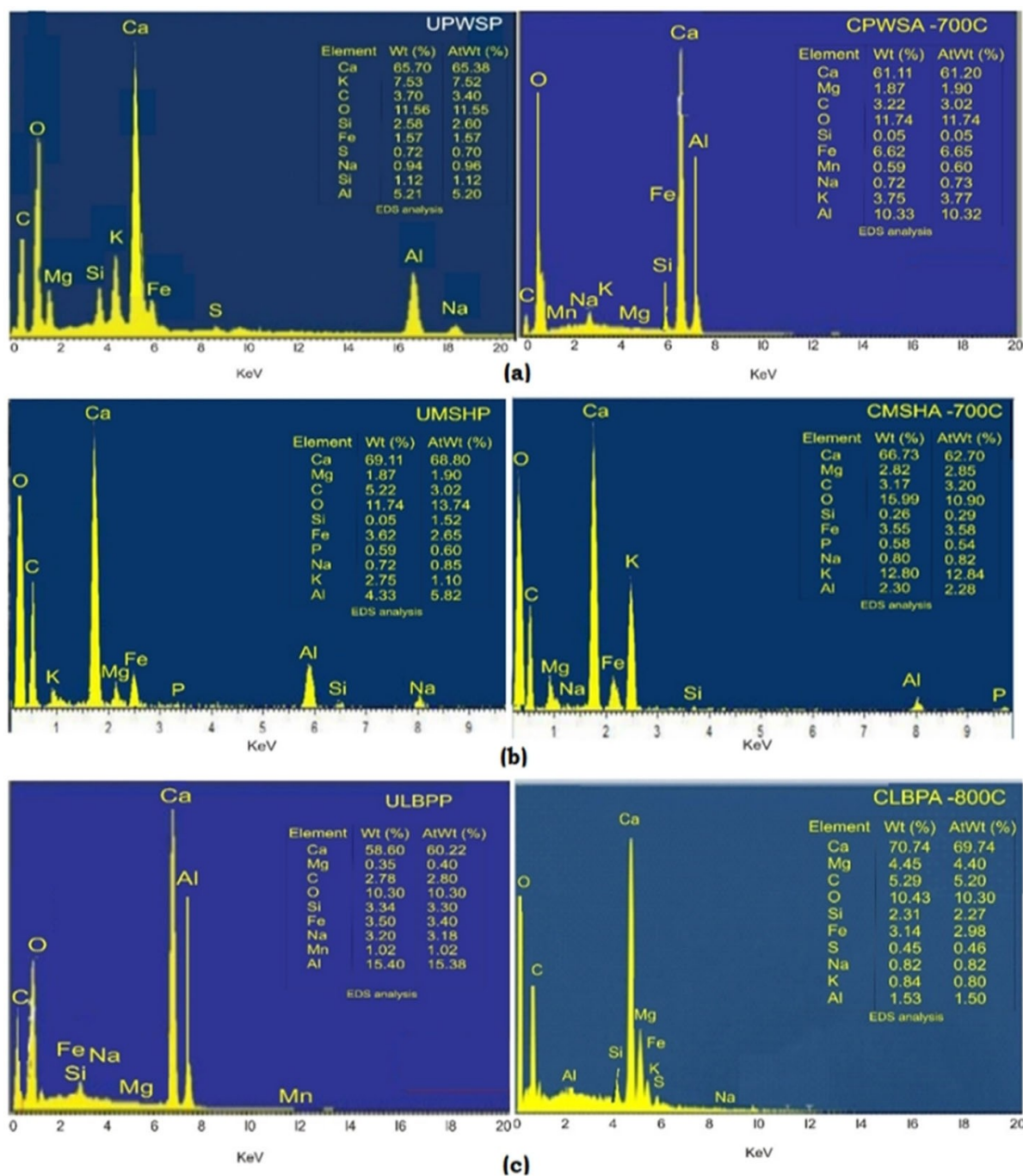
ChemistrySelect

Research Article
doi.org/10.1002/slct.202203816

Chemistry
Europe
European Chemical
Societies Publishing

Figure 1. EDS spectral showing the mass fraction of elements for both uncalcined and calcined ash samples of (a) UPWSP and CPWSA at 700 °C (b) UMSHP and CMSHA at 700 °C (c) ULBPP and CLBPA at 800 °C.

calcination temperature of 800 °C,[28] hence, the CPWSA catalyst was mass produced at 800 °C and used to produce biodiesel. Okoye et al.[25] reported a similar procedure for selecting the optimum calcination temperature for mass production of ash catalyst from oil palm empty fruit bunch. Hence, it was observed that calcination temperature significantly affects the crystalline phases present in both UPWSP and CPWSA.

XRD results of CMSHA catalyst at varying temperatures

The XRD patterns of UMSHP (raw sample) and CMSHA heterogeneous base catalysts investigated at different calcination temperatures (600-800 °C) are shown in Figure 3. It was observed that the XRD pattern of UMSHP has the main peak at 2θ of 22.10°, indicating the presence of a tetragonal crystal of SiO_2 (cristobalite), with lattice parameters $a = b = 4.988\ \text{Å}$ and $c = 6.970\ \text{Å}$ The values matched exactly
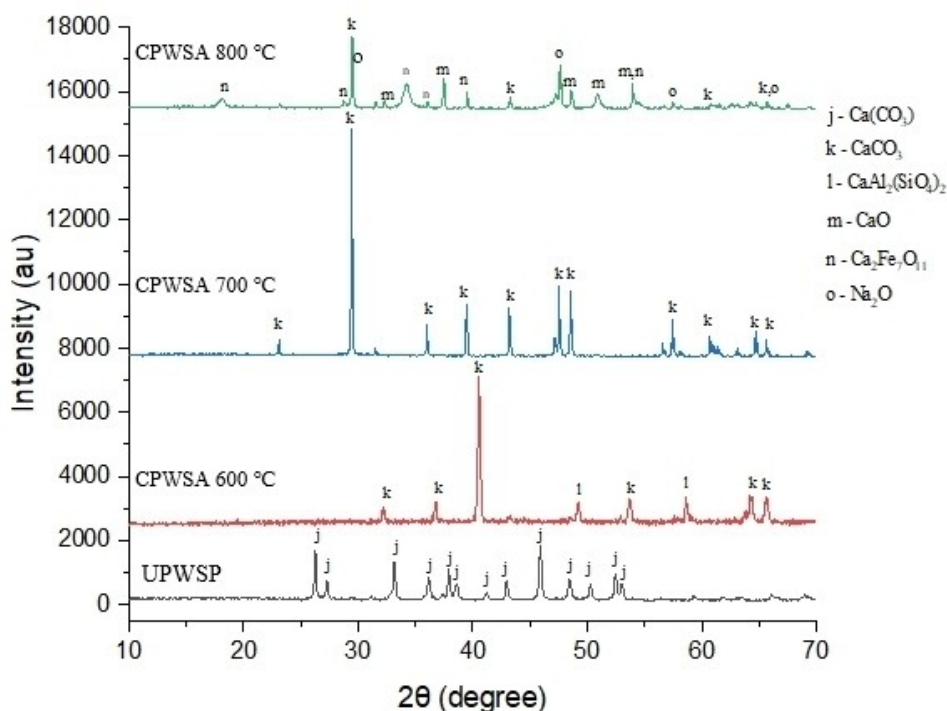
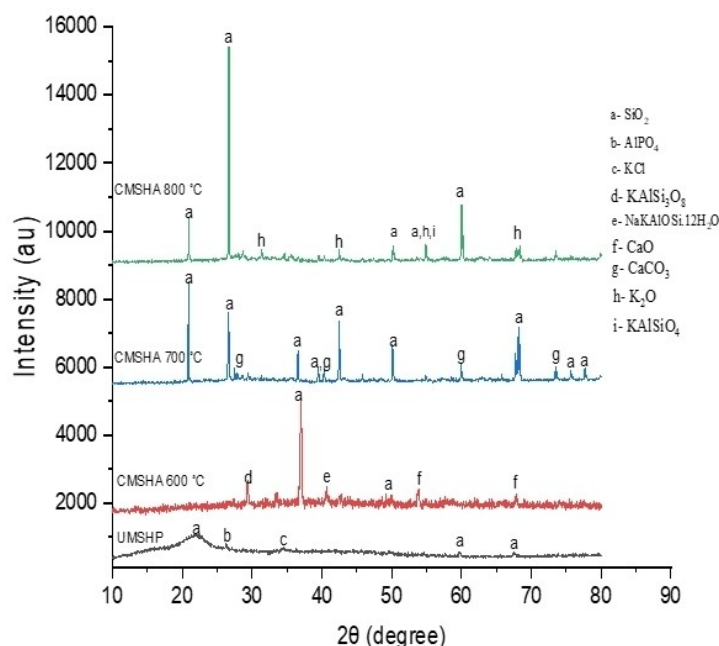**Figure 2.** XRD diffractograms of CPWSA catalyst at different temperatures.

Figure 3. XRD diffractograms of CMSHA catalyst at different temperatures.

with the standard data (JCPDS 01-077-1317). The other crystalline compounds present with low peaks were hexagonal crystals of aluminum phosphate ($AlPO_4$) at $2\theta = 26.39°$ and cubic crystals of potassium chloride (KCl) at $2\theta = 34.32°$ with JCPDS reference code 01–072-1064 and 01-077-2121, respectively. These compounds (SiO_2 and KCl) have been identified in other agricultural residues too. Mendonça et al.[24] reported the presence of KCl for *tucumã* peels at $2\theta = 29.50°$. According to Nath et al.,[19] the XRD peak in the *Brassica nigra* plant catalyst at $2\theta = 21.38°$ was as a result of the presence of silicon (IV) oxide, which is also known as a quart (SiO_2).

ChemistrySelect

Research Article
doi.org/10.1002/slct.202203816

Chemistry Europe
European Chemical
Societies Publishing

Evidently, from Figure 3, the main peaks at 2θ of 36.97°, 20.89° and 26.67° for the CMSHA catalysts at 600°C, 700°C and 800°C, respectively, were identified as hexagonal crystals of quartz (SiO_2) with JCPDS reference code 01-077-1317. This is supported by the result of the straw slag ash catalyst reported by Wang et al.,[37] where the XRD peak at 2θ of 34.43° confirmed the presence of SiO_2 (JCPDS reference code 89-3609) in the straw slag ash catalyst. At 600°C, small amount of hexagonal crystal of calcium oxide, CaO (JCPDS 00-001-0705), a tetrahedral sheet of vermiculite, $NaKAlOSi.12H_2O$, (JCPDS 00-005-0518) and microcline crystal of $KAlSi_3O_8$ (JCPDS 00-001-0705) were identified at 2θ of 53.85°, 40.67° and 29.43° respectively. The presence of these crystalline phases confirmed the EDX results which showed the appreciable composition of the alkaline metals (Ca, K, and Na) present.

Similar 2θ values of 33.32°, 37.18° and 66.60° for CaO were also reported for *Brassica nigra* catalyst calcined at 550°C[19] [23]. The presence of CaO was also reported for catalyst obtained from *Musa acuminata* peel with a comparable 2θ value by Pathak et al.[38] [42]. The rhombohedral crystalline phase of calcium carbonate, $CaCO_3$ (JCPDS 01-072-1937), was observed for calcination temperatures of 700°C, at 2θ of 40.28°, 59.98° and 73.44° with other crystalline phases of SiO_2 being the strong peak at this temperature. Betiku et al.[39] and Aleman-Ramirez et al.[20] detailed similar phases of $CaCO_3$ for kola-nut pod husk, and moringa leaves derived catalysts. At 800°C, potassium oxide, K_2O (JCPDS 01-077-0137) with a tetragonal crystalline phase was found at different peaks at 2θ of 26.78°, 31.38°, 42.51°, 54.91° and 68.35°. At that temperature, it becomes the major phase, and main peak next to SiO_2 (Figure 3) The hexagonal crystalline phase of potassium aluminum silicate, $KAlSiO_4$, (Kalsilite, JCPDS 01-076-0635) was also observed at 2θ of 55.04°. Nath et al.[23] reported the presence of K_2O in *Brassica nigra* plant ash catalyst calcined at 550°C with comparable 2θ value at 27.80°, 39.52°, 46.70° and 48.12°. In addition, Okoye et al.[30] similarly observed the hexagonal crystalline phase of kalsilite, $KAlSiO_4$ (ICSD 00-012-0134) at 2θ of 29.10° in oil palm empty fruit bunch ash catalyst. Hence, the basic sites ($KAlO_2$) in $KAlSiO_4$ are gotten from the interface between the K^+ and aluminum oxide.

As a result, the XRD pattern of CMSHA catalyst at different calcination temperatures confirmed the existence of inorganic chemical combinations. At various calcination temperatures, K, Ca, and Na were the principal metallic elements discovered in various forms of crystalline compounds and supported by the EDX study. Thus, when the calcination temperature was less than 800°C, the CMSHA catalyst's composition was dominated by SiO_2. The peaks of metallic phases of K_2O were dominating at 800°C. This temperature is proposed as the ideal temperature for mass production of the ash catalyst from melon seed husk. Muciño et al.[40] proposed a similar approach for determining the optimal temperature for bulk production of ash catalyst from sea sand.

XRD results of CMSHA catalyst

Figure 4 depicts the XRD patterns of uncalcined locust bean pod-husk, ULBP, and CLBPA catalysts studied at various calcination temperatures. The ULBP XRD pattern consists mostly of cubic crystalline sodium aluminum-silicate-bromide ($Na_8(Al_6Si_6O_{24})$ Br_2) with lattice parameters $a = b = c = 8.930$ Å, as evidenced by the predominant diffraction peak at $2\theta = 24.37°$ and matched with JCPDS reference number 01-080-1133. At $2\theta = 14.99°$, Quart (SiO_2) phase was also discovered. Akpenpuun et al.[41] and Olubajo et al.[23] reported the presence of SiO_2, Al_2O_3 and Na_2O in the calcined ash sample of locust bean pod (LBP). Hence, it could be inferred that these compounds ($SiO_2 + Al_2O_3 + Na_2O$) exist in the cubic phase of $Na_8(Al_6Si_6O_{24})$ Br_2 in the raw sample of LBP with bromine probably vapourised away due to higher temperature above its boiling point of 58.8°C.

The hexagonal crystalline phase of SiO_2 (JCPDS 01-085-0794) showed the sharp peak identified at $2\theta = 37.18°$ *and* 29.62° in the LBPA calcined at 600°C. The crystalline phases of microcline, $KAlSi_3O_8$ (JCPDS 00-001-0705) and anorthite, $CaAl_2(SiO_4)_2$, (JCPDS 00-002-0523) were also identified at 2θ of 33.64°, 38.83°, 46.66° and 45.58° respectively. Ekeoma et al.[36] has identified this compound in clay formulation catalyst for biodiesel production, which is one of the most commonly heterogeneous catalysts as reported by Etim et al..[28] The formation of microcline ($KAlSi_3O_8$) and anorthite ($CaAl_2(SiO_4)_2$) may be due to the heat application at this temperature (600°C).

The CLBPA catalyst at 700°C indicated the presence of three compounds namely fairchildite ($K_2Ca(CO_3)_2$), Magnesite ($MgCO_3$) and potassium-sodium-chromium oxide ($K_3Na(CrO_4)_2$. The fairchildite with JCPDS reference code 00–021-0981 was identified with a hexagonal crystalline phase with lattice parameters $a = b = 5.290$ Å and $c = 13.320$ Å Also, fairchildite ($K_2Ca(CO_3)_2$) was indicated by the diffraction peaks 2θ of 13.42°, 20.72°, 26.86°, 28.12°, 34.03° and 40.72°. Fairchildite compound was discovered in 1947 in the western United States from wood ashes, according to Aleman-Ramirez et al.,[20] and it has been found in agricultural residues. This chemical compound was also discovered in moringa leave powder calcined at 500°C as a sustainable precursor for biodiesel production by Aleman-Ramirez et al..[20]

The diffraction peaks for $MgCO_3$ (JCPDS 01-082-0538) were indicated at $2\theta = 33.35°$, 39.62° *and* 60.10° and were identified with a rhombohedral crystalline phase. Similarly, Muciño et al.[44] reported the presence of $MgCO_3$ with JCPDS 02-08-71 in the sea sand calcined at 700°C as a potential heterogeneous catalyst for biodiesel synthesis. Correspondingly, the diffraction peaks for $K_3Na(CrO_4)_2$ (JCPDS 00-003-0773) were shown at $2\theta = 29.54°$, 30.48° *and* 62.52° and were identified with a monoclinic crystalline phase. The XRD patterns of CLBPA at 800°C showed major diffraction peaks of magnesium oxide, MgO (JCPDS 01-077-2364) identified with a cubic crystalline phase ($a = b = c = 4.209$ Å) at $2\theta = 42.98°$, 62.44° *and* 78.65°. This implied that the magnesite ($MgCO_3$) phase identified at 700°C has thermally decom-
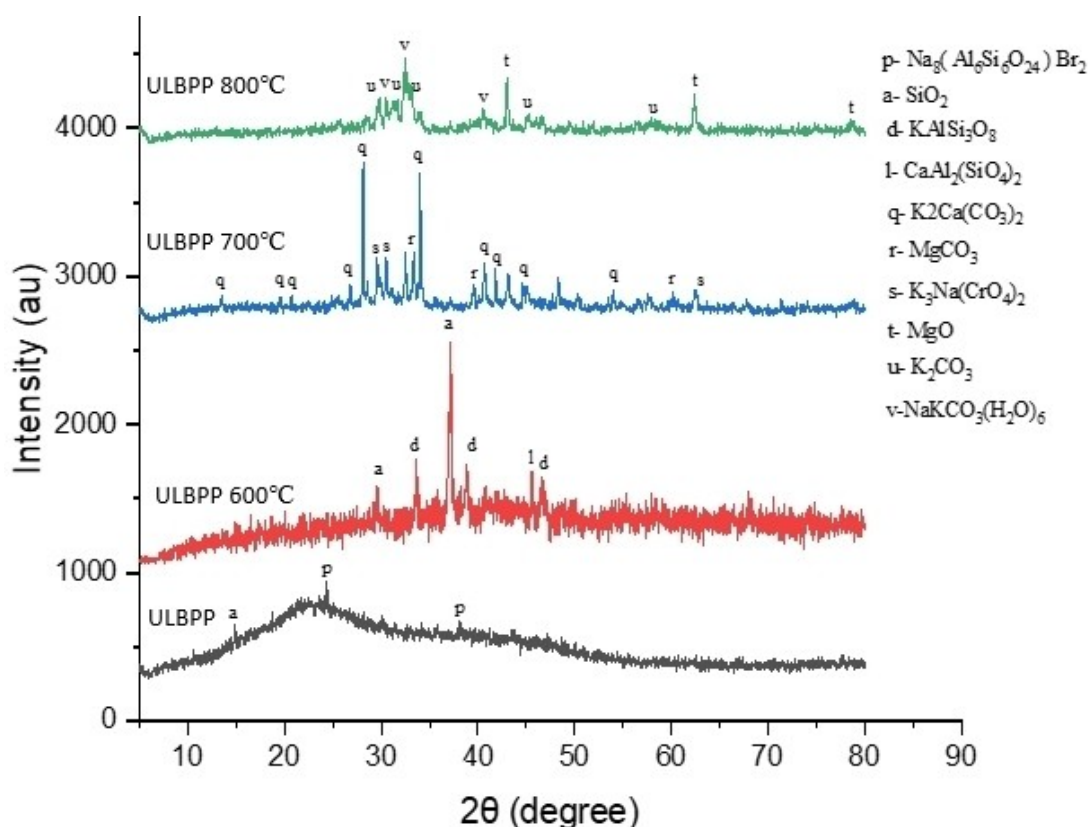
Figure 4. XRD diffractogram of CLBPA catalyst at different temperatures.

posed into MgO (Magnesium oxide). Muciño et al.[40] conveyed comparable transformation for magnesite in calcined sea sand heterogeneous catalyst where $MgCO_3$ was completely transformed into MgO at 700 °C.

Moreover, the diffraction peaks of potassium carbonate, K_2CO_3 (JCPDS 01-070-0292) were observed at 2θ of 30.54°, 32.41° and 40.54°. The K_2CO_3, was identified with monoclinic crystalline phase with lattice parameters $a = 5.675$ Å, $b = 9.920$ Å and $c = 7.018$ Å This crystalline phase has been identified in plant ashes. A study conducted by Etim et al.[28] and Nath et al.[19] 23 identified the presence of K_2CO_3 in calcined ripe plantain fruit peel and *Brassica nigra* plant ashes. The sodium- potassium-carbonate-hexahydrate ($NaKCO_3.6H_2O$; JCPDS 01-084-0638) was recognized with a monoclinic crystalline phase at diffraction peaks of $2\theta = 30.53°$, 32.45° and 40.54°. Therefore, at different calcination temperatures, K, Ca, Mg and Na were the major metallic elements which were found in different forms of crystalline compounds.

Hence, the results of the EDX analysis supported the view that K, Ca, Mg and Na were the main alkaline elements present in CPWSA, CMSHA and CLBPA. Hence, they could be used as biobased heterogeneous catalysts in biodiesel production. Etim et al.[28] and Betiku et al.[39] testified that the oxide from these metallic elements (alkaline elements) had been shown to have high catalytic behaviour in biodiesel production. In this study, an optimum temperature of 800 °C was recommended for the

mass production of each of these catalysts. Based on the phase identification and scoring of this alkaline metallic oxide as analyzed by XRD, further characterization of these potential catalysts was done using the CPWSA, CMSHA and CLBPA at 800 °C.

Fourier Transform Infrared (FTIR) analyses

The Fourier transform infrared (FTIR) analysis was done to identify the functional group present in the samples. This was observed for the raw and calcined catalyst at optimum calcination temperature (800 °C), which showed the crystalline phases majorly with high potential catalytic behaviour in biodiesel production.

FTIR patterns of UPWSP and CPWSA catalyst at 800 °C

The FTIR pattern of both UPWSP and CPWSA catalysts at 800 °C was presented in Figures 5a-b. In UPWSP (Figure 5a), the strong peak at 1560.86 cm^{-1} shows a band that represents the C=O group in CO_3^{2-}. Boonyuen et al.[34] 39 also identified the presence of C=O group in the uncalcined sample of *Turbo jordani* shells. The other characteristics of absorption peaks positioned at 3542.11, 2582.88, 720.19, and 880.10 cm^{-1} represent the stretching vibrations of C–O group also in CO_3^{2-} which suggests the presence of aragonite. Lee et al.,[42] and Olatundun et al.[31] reported similar C–O stretching for cocoa pod-husk plantain

ChemistrySelect

Research Article
doi.org/10.1002/slct.202203816

Chemistry Europe
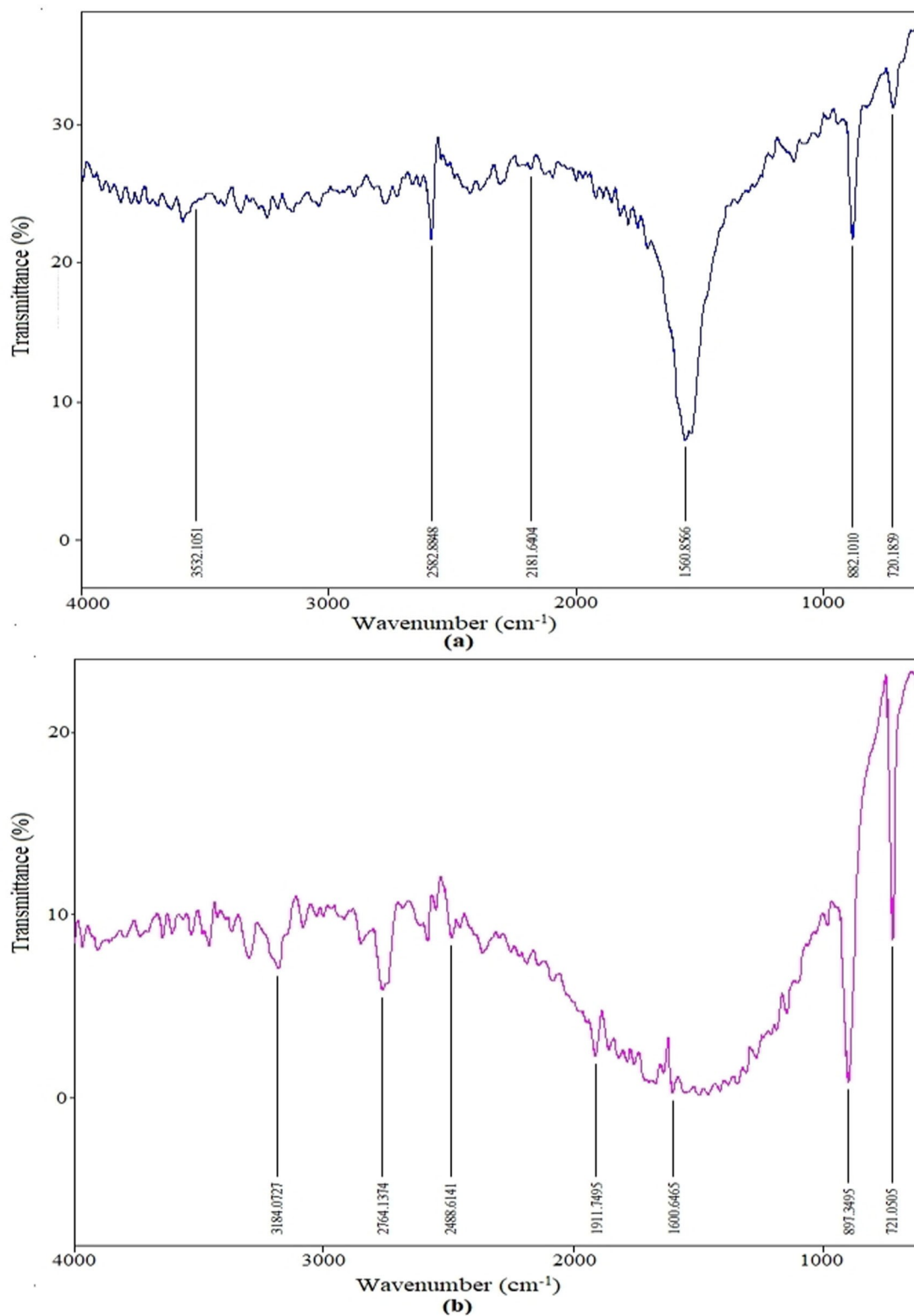European Chemical
Societies Publishing

Figure 5. FTIR spectra of (a) UPWSP (b) CPWSA at 800 °C.

peel blend and pure aragonite seed, respectively. In the CPWSA catalyst at 800°C (Figure 5b), the peaks at 721.05, 897.35, and 1600.65 cm^{-1} are due to the stretching vibrations of Ca—O and Na—O bonds, suggesting the presence of CaO and Na$_2$O in the CPWSA catalyst. A similar observation was detailed by Nath et al.[19] for the calcined *Brassica nigra* ash catalyst, which

ChemistrySelect

Research Article
doi.org/10.1002/slct.202203816

Chemistry Europe
European Chemical
Societies Publishing

showed the stretching vibration of Ca—O and K—O bonds at IR peak of 624 cm^{-1}. The peak at 1911.75 cm^{-1} was associated with the C—O bond of metal carbonates, which may be formed due to the CO_2 absorption onto the surface of the metal oxide of CPWSA at 800 °C; which implies the presence of Ca, Na and metal carbonate suggesting $CaCO_3$ and Na_2CO_3. A similar band was reported for the ash catalyst developed from banana peels by Betiku et al.[17] and *Tectona grandis* leaves by Gohain et al.,[43] which reported a C—O bond of metal carbonates at 1654, 1389 and 870 cm^{-1} for the ash catalyst. The peak at 2764.14 cm^{-1} may be attributed to Ca-O—Fe bonds stretching vibrations that may be due to the presence of $Ca_2Fe_7O_{11}$ in the CPWSA catalyst.

The peak at 3184.07 cm^{-1} was caused by the presence of O—H vibration, which might be caused by water molecules absorption on the surface of the CPWSA catalyst at 800 °C. Betiku et al.[39] observed comparable stretching vibrations for a heterogeneous base catalyst made from kola nut pod husk, with the peak at 3200 cm^{-1} attributed to the stretching and bending vibration of the O—H group present in the calcined ash catalyst of kola nut pod husk. As a consequence, the FTIR spectra for both the UPWSP and CPWSA catalysts matched with the XRD data, confirming the presence of metal oxides and carbonate in the catalyst.

FTIR patterns of UMSHP and CMSHA catalyst

The FTIR spectra for both UMSHP and CMSHA at 800 °C were presented in Figures 6a&b. In the analysis of the UMSHP (Figure 6a), the peak at 3259.91 cm^{-1} in the spectrum was associated with the bending and stretching vibration of the O—H group, which has been reported to be due to the adsorbed water molecules on the surface of the UMSHP sample.[3,19] The asymmetric vibrations of the O—H group were also identified in the CMSHA catalyst (Figure 6b) at the peaks of 3788, 3142, 2756, and 1492 cm^{-1}, respectively. This suggests a transformational phase of the constituent metal ions in the catalysts to oxide, confirming the presence of KO_2 in the
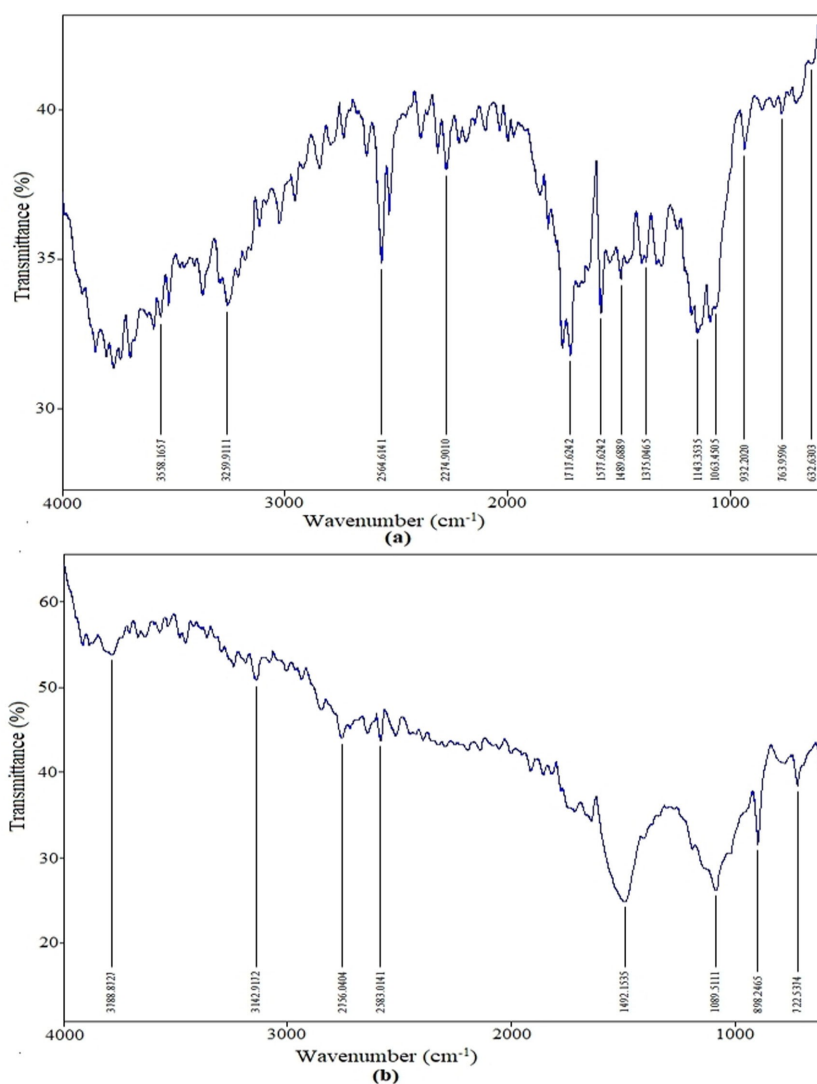

Figure 6. The FTIR spectra of (a) UMSHP (b) CMSHA at 800 °C.

catalyst. The bonds at 2564.61 and 2274.90 cm^{-1} (Figure 6a) showed the asymmetric stretching vibration of C—H in the —CH$_2$ group. Etim et al.[18] stated that the peaks at 2920 and 2850 cm^{-1} identified in ripe plantain peel-derived catalysts were attributed to the strong asymmetric stretching vibration of —CH$_2$ and strong symmetric stretching vibrations of —CH$_2$, respectively. In addition, the peaks at 1577 and 1717 cm^{-1} were associated with the asymmetric stretching vibrations of C=O bonds of metal carbonate.

Likewise, the peaks at 1489, 1375, 1143, and 1063 cm^{-1} (Figure 6a) are assigned to carbonate bending vibrations of the C—O group. The presence of a band corresponding to —SiO and —PO$_4$ was also noticed, which may be agitated by contact with Al^{3+} at 1063 cm^{-1}. Mendonça et al.[24] reported similar bands for *tucumã* peels at peaks of 1000 and 1107 cm^{-1}, corresponding to phosphate and silicate presence. The peaks at 932, 763, and 632 cm^{-1} may be due to Si—O—Si and K—Cl symmetric vibrations suggesting the presence of SiO$_2$ and KCl in the UMSHP (Figure 6a). Etim et al.[18] reported the presence of similar asymmetric stretching vibrations of Si—O—Si at the peak of

1005 cm^{-1} for the ripe plantain fruit peels. The spectral of CMSHA$_{800°C}$ at the peak of 1089 cm^{-1} may be owing to the -SiO alternating to -AlO stretching and bending plane of the catalyst, which may be agitated by contact with K$^+$. Thus, signifying the presence of KAlSiO$_4$. Okoye et al.[25] also stated a similar vibration peak around 1032 cm^{-1} which was due to the stretching vibration of K—Al—Si—O. The bonds at 898 and 722 cm^{-1} were features of -SiO$_4$ isolated vibration in Ca$_3$Al$_2$Si from interaction with Al^{3+} and Ca^{2+}. Similar interactions have been reported for the calcined ash catalyst prepared from *tucumã* peels by Mendonça et al.,[24] which shows that the catalyst's IR spectral at the peak of 864 cm^{-1} characterized the SiO$_4$ vibration in CaMgSiO$_4$. Hence, the IR spectral for both UPWS and CPWSA catalysts at 800°C were agreed with the results from the XRD analysis.

FTIR patterns of ULBPP and CLBPA catalyst at 800°C

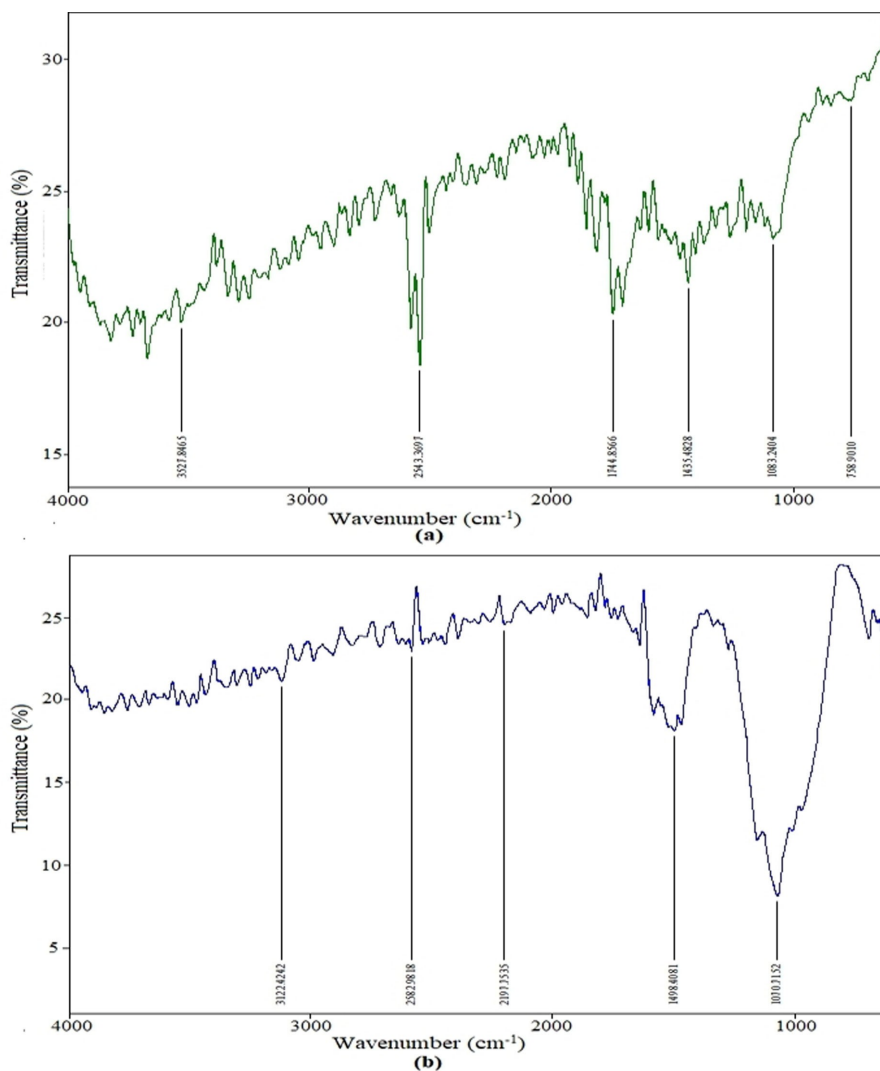The infrared spectrum of the ULBPP and CLBPA catalyst at 800°C were shown in Figure 7a-b with various adsorption

Figure 7. The FTIR spectra of (a) ULBP (b) CLBPA at 800°C.

ChemistrySelect

Research Article
doi.org/10.1002/slct.202203816

Chemistry Europe
European Chemical
Societies Publishing

bands. The weak peak at 3527 cm^{-1} and the strong peak at 2543 cm-1 in ULBP (Figure 7a) were attributed to the C—H functional group's asymmetric bending and trenching vibrations in the —CH$_2$ group. Etim et al.[18] stated that the peaks at 2920 and 2850 cm^{-1} identified in ripe plantain peel were attributed to the strong asymmetric stretching vibration of -CH$_2$ and strong symmetric stretching vibrations of —CH$_2$, respectively. The peak at 1744 and 1435 cm^{-1} represents the C=O stretching vibration of metal carbonate that may be formed because of the adsorption of CO$_2$ to the surface of metal oxide [47]. The peaks at 1083 cm^{-1} may be due to Si—O—Si bonds suggesting the presence of SiO$_2$. Similar asymmetric stretching vibrations of Si—O—Si at the peak of 1005 cm^{-1} were detailed by Etim et al.[18] for ripe plantain peels. The minor band at 758 cm^{-1} could be ascribed to the -OH stretching and binding vibration of the water molecule.

A similar observation was reported for *Musa acuminata* peduncle at the IR spectral peak of 666 cm^{-1}.[44] Figure 7b shows the IR spectra for the CLBPA catalyst. The significant peaks at 1070 and 1498 cm^{-1} were associated with the C—O bond of metal carbonates which may be formed due to the CO$_2$ absorption to the surface of CLBPA metal oxide.[28,31] The perceived traces of Mg, Na, and metal carbonate suggests the presence of K$_2$CO$_3$, Mg—O and CO_3^{2-}, which may be agitated with Na$^+$ and K$^+$ in NaKCO$_3$.6H$_2$O present in CLBPA catalyst. A similar band was reported for the ash catalyst developed from banana peels by Betiku et al.,[17] and *Tectona grandis* leaves by Gohain et al.,[43] who reported a C—O bond of metal carbonates at 1654, 1389, and 870 cm^{-1} for the ash catalyst. The weak peaks at 3122, 2582, and 2197 cm^{-1} may be attributed to the C=O.

Basicity characteristics of CPWSA, CMSHA, and CLBPA catalyst at 800 °C

The basicity of heterogeneous catalysts plays a vital role in the behavior of catalysts during transesterification reaction.[20,24] The basicity of CPWSA, CMSHA and CLBPA at an optimum calcination temperature of 800 °C was determined following a method described by Nath et al..[19] 1.0 g of each of the catalyst samples was dissolved in 10 ml of water, shaken vigorously and allowed to stand for 10 minutes. The pH of the aqueous solution was then determined via a pH meter. The basicity of the CPWSA, CMSHA and CLBPA showed an average pH value of 11.65, 10.41 and 11.62, respectively. The obtained pH values represent the high basic nature of the catalysts, making them potential heterogeneous biobased catalysts for renewable biodiesel production. The high basic nature of the catalysts may be due to the presence of alkaline elements in each of the calcined ash samples, as confirmed by EDX analysis. This might have positively contributed to the yield of Palm Kernel Oil Ethyl Ester (PKOEE) during the production process. Nath et al.[19] observed a similar result for the basicity of *Brassica nigra* plant-derived catalyst with a pH value of 11.91 when 1.0 g of the ash sample was dissolved in 5 ml of water. However, the basicity of *Brassica nigra* plant derived catalyst is higher than the pH values of the three potential catalysts.

Basicity characteristics of CPWSA, CMSHA, and CLBPA catalyst at 800 °C

As mentioned earlier, the basicity of heterogeneous catalysts plays a vital role in the behaviour of catalysts during transesterification reaction .[20] The basicity of CPWSA, CMSHA and CLBPA at an optimum calcination temperature of 800 °C was determined following a method described by Nath et al..[19] 1.0 g of each of the catalyst samples was dissolved in 10 ml of water, shaken vigorously and allowed to stand for 10 minutes. The pH of the aqueous solution was then determined via a pH meter. The basicity of the CPWSA, CMSHA and CLBPA showed an average pH value of 11.65, 10.41 and 11.62, respectively. The obtained pH values represent the high basic nature of the catalysts, making them potential heterogeneous biobased catalysts for renewable biodiesel production. The high basic nature of the catalysts may be due to the presence of alkaline elements in each of the calcined ash samples, as confirmed by EDX analysis. This might have positively contributed to the yield of Palm Kernel Oil Ethyl Ester (PKOEE) during the production process. Nath et al.[19] observed a similar result for the basicity of *Brassica nigra* plant-derived catalyst with a pH value of 11.91 when 1.0 g of the ash sample was dissolved in 5 ml of water. However, the basicity of *Brassica nigra* plant derived catalyst is higher than the pH values of the three potential catalysts.

Catalytic testing of CPWSA, CMSHA and CLBPA via PKO transesterification

The catalytic strength of each of the ash (catalyst) samples were tested via transesterification of palm kernel oil and ethanol at reaction conditions of the ethanol-to-oil ratio of 6:1, catalyst loading of 7.0 wt.%, reaction temperature of 65 °C and reaction time of 120 min. At the end of the reaction, it was observed that the three calcined ash samples (CPWSA, CMSHA, and CLBPA catalysts) produced golden yellow biodiesel from PKO (Figure 8). The CPWSA catalyst had a PKOEE yield of 84.38%, CMSHA, and CLBPA catalysts produced a moderate PKOEE yield of 34.63 and 40.54%, respectively. The moderate PKOEE yield of CMSHA and CLBPA could be attributed to the reaction conditions used, such as catalyst loading and reaction time. It may be that if catalyst loading and the reaction time are increased, an appreciable biodiesel yield can be obtained using CMSHA and CLBPA. Improving any of these reaction conditions might improve the biodiesel yield.[19] Okoye et al.[21b] reported a similar comparable biodiesel yield of 73.92% for a calcined periwinkle shell at 400 °C when used for transesterification of waste cooking oil. The ability of CPWSA, CMSHA and CLBPA catalysts to produce biodiesel from PKO, is an indication that they can be used as heterogeneous catalysts in biodiesel production.
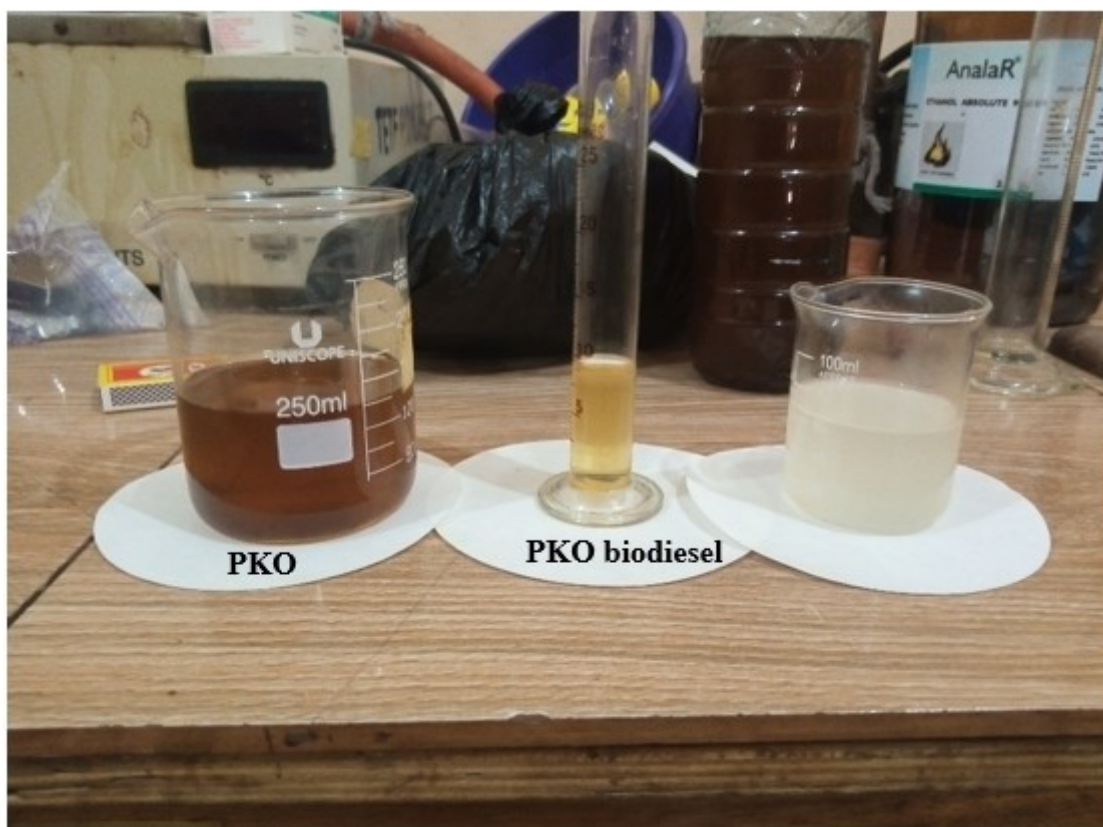
Figure 8. PKO biodiesel sample.

Relationship between the structure and catalytic performance of CPWSA, CMSHA and CLBPA

To summarize the characterization data mentioned above, the catalyst thermally decomposes during calcination, resulting in the generation of metal oxides and mixed metal oxides. On the other hand, the optimal calcination temperature of 800 °C provided the metal oxides responsible for the catalytic performance of each heterogeneous base catalyst. At 800 °C, the CPWSA, CMSHA, and CLBPA derived heterogeneous base catalysts were employed for palm kernel oil transesterification (PKO). The CPWSA catalyst's catalytic activity is mostly attributable to the $Ca^{2+}-O^{2-}$ and $Na+-O^{2-}$ ions, whereas CMSHA and CLBPA at the same temperature are assigned to the $K+-O^{2-}$ and $Mg+-O^{2-}$ ions, respectively. As a result, these metal oxides are thought to be the primary catalytic sites for the transesterification reaction. These metal oxides' activity in transesterification reactions for various calcined ash produced heterogeneous base catalysts has been reported by Oloyede et al..[45] The catalyst stability during reusability also may be due to the formation of C–O, C=O, Ca–O, Na–O, and Mg–O bonds in the catalysts. Xie and Zhao[8] reported similar activity for the CaO-MoO$_3$-SBA-15 heterogeneous catalyst.

CPWSA, CMSHA and CLBPA reusability studies

The CPWSA, CMSHA, and CLBPA were tested for reusability under reaction conditions of 6:1 ethanol-to-oil ratio, 7.0 wt.% catalyst loading, 65 °C reaction temperature, and 120 min reaction duration. The results of this study is presented in Figure 9. The product mixture and the catalyst were separated after each transesterification cycle by filtration using Whatman filter paper 110 microns. The catalyst was reused without any additional treatment, such as washing or calcination.[19,27] The biodiesel yield of the CPWSA, CMSHA, and CLBPA decreased from 84.38, 34.63, and 40.54 %, respectively, at the conclusion of the third cycle to 83.67, 32.45, and 39.12 %, respectively. The reduction in the values of PKOEE yield could be credited to the loss of part of the catalyst as well as the leaching of active metals from the surface of the catalysts.[27] As a result, the catalysts displayed significant catalytic activity when reutilized for transesterification and are heterogeneous in nature due to their recoverability and reusability. Similar catalytic behavior in biodiesel yield during reusability was also observed by Yin et al.[13c] and Falowo et al..[27]

Fuel properties of PKOEE

Table 3 depicts the fuel parameters of PKOEE samples generated utilizing CPWSA, CMSHA, and CLBPA as catalysts for
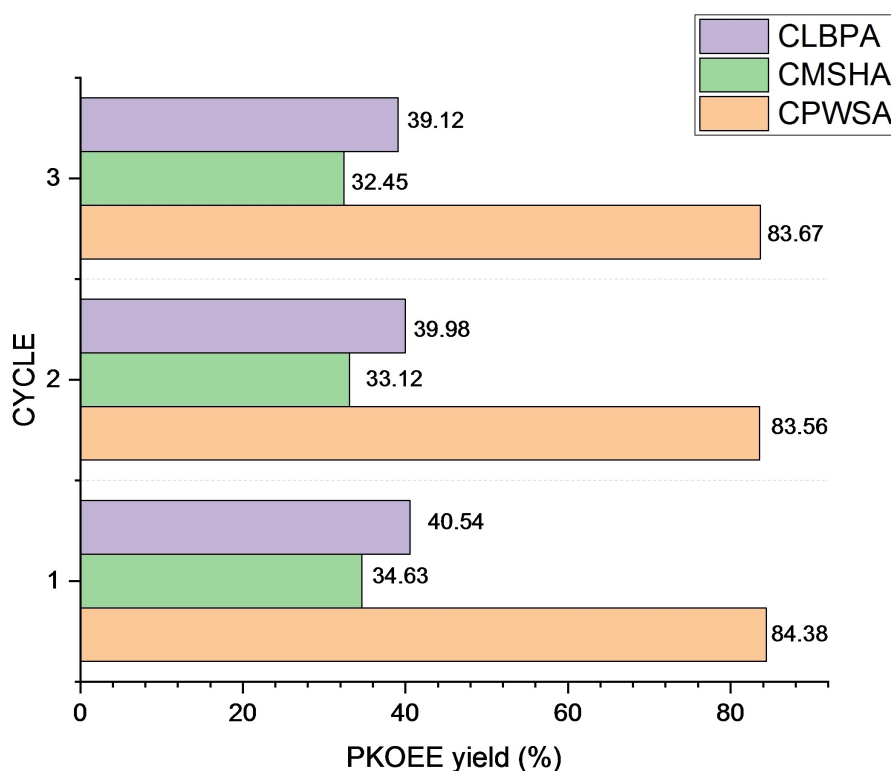
ChemistrySelect

Research Article
doi.org/10.1002/slct.202203816

Chemistry Europe
European Chemical
Societies Publishing

Figure 9. Catalyst reusability vs. PKO biodiesel yields.

Table 3. Fuel properties of the PKO biodiesel produced during CPWSA, CMSHA, and CLBPA catalyzed transesterification.

PKO Biodiesel Fuel properties	Unit	CPWSA	CMSHA	CLBPA	Test method	ASTM-D6751 Biodiesel Standard
Kinematic viscosity at (40°C)	mm^2/s	4.5	5.1	4.8	D455	1.9–6.0
Specific gravity		0.872	0.880	0.850	D4052	0.86–0.9
Flash point	°C	218	185	235	D93	93–130
Cloud point	°C	+7	+6	+9	D2500	NR
Iodine value	GI$_2$ 100 g^{-1}	72.1	89.0	75.5	D664 11	NR
Saponification Value	Mg KOH	120.4	115.6	130.4	NR	NR
Cetane number		30.53	73.49	71.18	D613	51–47
Calorific value	MJ kg^{-1}	8.54	9.19	8.91	NR	NR
Pour point	°C	+4.0	+3.0	+5.0	D97	NR
[NR]: Not Reported.						

the transesterification reaction. Biodiesel samples produced using CPWSA, CMSHA, and CLBPA as catalysts had kinematic viscosities of 4.5, 5.1, and 4.8 mm^2/s, respectively. Akhabue and Ogogo[46] and Odude et al.[30] also reported similar values of 4.64, 4.7, and 4.3 mm^2/s for the kinematic viscosity of palm kernel oil methyl esters (PKOME) using heterogeneous catalyst derived from calcined hen-eggshell, calcined banana peel ash (CBPA) and calcined cocoa pod-husk ash (CCPHA), respectively. Furthermore, the kinematic viscosities of the biodiesel samples in this investigation are extremely close to previously published values of 4.84 mm^2/s, and 5.0 mm^2/s for PKOME generated utilizing potassium hydroxide (PKO) as a homogeneous base catalyst by Alamu et al.[47] and Odude et al..[30] This demon-

strates that the kinematic viscosity values found in this investigation are consistent with previously published values in similar experiments. During the CPWSA, CMSHA, and CLBPA-catalyzed transesterification reaction, the specific gravity of the PKO biodiesel samples is 0.872, 0.880, and 0.850, respectively.

The flash points of 218, 185, and 235°C, cloud points of +7, +6, and +9°C, and pour points of +4, +3, and +5°C were obtained for the PKOEE using CPWSA, CMSHA, and CLBPA, respectively. This submits that the biodiesel produced was safe to handle and store.[30] The high value of the flash point of PKOEE may be due to the major presence of 9-octadecenoic and dodecanoic acids (C$_{18}$H$_{34}$O$_2$ and C$_{12}$H$_{24}$O$_2$) in the PKOEE.[27] The obtained values for the flash points, cloud points, and pour

ChemistrySelect

Research Article
doi.org/10.1002/slct.202203816

Chemistry Europe
European Chemical
Societies Publishing

Table 4. Fatty acid composition of PKOEE using CPWSA, CMSHA and CLBPA.

Composition (wt.%)

Fatty acid esters	Formula	CPWSA	CMSHA	CLBPA	CPA[26]	CBPA[30]	CCPHA[30]
Ethyl nonanoate	$C_{11}H_{22}O_2$	NF	0.06	0.6	0.34	NR	NR
Ethyl octanoate	$C_{10}H_{20}O_2$	3.96	3.93	3.95	2.52	3.6	3.6
Ethyl hexadecanoate	$C_{18}H_{36}O_2$	0.83	0.85	0.78	4.93	8.3	8.0
Ethyl tetracosanoate	$C_{26}H_{52}O_2$	0.09	0.08	0.08	NR	0.2	0.1
Ethyl decanoate	$C_{12}H_{24}O_2$	1.5	2.3	1.9	3.10	2.3	2.4
Ethyl pentadecanoate	$C_{17}H_{34}O_2$	1.2	1.1	2.1	9.97	NR	NR
Ethyl dodecanoate	$C_{14}H_{28}O_2$	38.6	36.3	44.05	19.41	41.8	43.1
Ethyl octadecanoate	$C_{20}H_{40}O_2$	8.5	7.3	8.01	9.74	3.7	9.4
Ethyl tetradecanoate	$C_{16}H_{32}O_2$	0.6	2.3	0.95	NR	19.1	13.5
Ethyl elaidate	$C_{20}H_{38}O_2$	43.05	45.21	35.9	NR	16.3	14.1
Ethyl behenate	$C_{24}H_{48}O_2$	0.2	0.1	0.5	NR	0.4	0.2
Ethyl-9-hexadecenoate	$C_{18}H_{34}O_2$	0.43	0.07	0.19	4.93	0.7	0.3
Ethyl-9,12-octadecadienoate	$C_{20}H_{36}O_2$	0.9	NF	1.3	NR	0.8	0.3

PKOEE used in present study, whereas PKOME was used in previous studies. [CPA]: Cocoa Pod Ash, [NF]: Not found, [NR]: Not reported.

points of PKO biodiesel samples produced are very close to the reported value of 167 °C, +6 °C, and +2 °C, respectively, for PKO biodiesel produced by Alamu et al.[47] using KOH catalyzed transesterification with ethanol. The cetane numbers 30.53, 73.49, and 71.18 were observed for PKOEE obtained with CPWSA, CMSHA, and CLBPA, respectively. The cetane number, specific gravity, kinematic viscosities, and calorific value of PKOEE indicate that the biodiesel produced will provide good ignition quality and enough energy when utilized in compression ignition engines.[48] The obtained cetane number values agree with PKOME values of 44.4 and 76.93, employing CBPA and CCPHA as catalysts, respectively.[30] Except for the flash point and cetane number for the biodiesel samples obtained via the CMSHA and CLBPA catalyzed transesterification process, all of the characteristics were within the ASTM D6751 standard.

Chemical compositions of PKOEE

The chemical composition of PKOEE synthesized as analyzed via GC is listed in Table 4. The methyl esters found in the PKOEE from CPWSA catalyzed transesterification reaction was primarily ethyl elaidate (43.05%), ethyl dodecanoate (38.6%), ethyl octadecanoate (8.5%), and ethyl octanoate (3.96%). Those observed in CMSHA-catalyzed transesterification reaction composed of ethyl elaidate (45.21%), ethyl dodecanoate (36.3%), ethyl octadecanoate (7.3%), and ethyl octanoate (3.93%). In contrast, those seen in the CLBPA-catalyzed transesterification reaction include ethyl dodecanoate (44.05%), ethyl elaidate (35.9%), ethyl octadecanoate (8.01%), and ethyl octanoate (3.95%). The results showed that the composition of PKOEE produced utilizing the CPWSA, CMSHA, and CLBPA was highly saturated, which is consistent with what has been reported for PKOMEE and PKO by Aladetuyi et al.,[26] Odude et al.[30] and Betiku et al..[17]

Cost analysis of the developed CPWSA, CMSHA and CLBPA

The cost of the catalyst employed in the transesterification process significantly impacts the cost of biodiesel generation.[41,49] The current study concentrated on the possible utilization of three new heterogeneous base catalysts for oil transesterification into biodiesel. As a result, the cost evaluation of the catalyst developed from the three selected agricultural residues is critical to certify its marketability in the transesterification process. The overall cost of the three developed catalysts is impacted by various characteristics such as collection source and preparation methods. The cost calculation at different levels and their combinations determines the marketability of such low-cost catalysts. The cost of making 1000 g of each developed heterogeneous base catalyst in different processes was computed in Nigeria naira (N) and US Dollars as discussed below:

Cost of Starting Materials (selected agricultural residues), (CSM) = N 0.00k/$0.00 (the starting materials are naturally available and are treated as wastes)

Cost of each unit operation for the production of CPWSA, CMSHA, and CLBPA

Washing Cost of the Starting Materials (WCSM) = N 2000/$5 (The selected residues were washed with tap water followed by distilled water. The distilled water was purchased at the rate of N 80.00k/$0.20 per litre, and 25 L was used).

Drying Cost of the starting materials (DCSM):

$$DCSM = \ unit \times \frac{cost}{unit} \times hour = 1 \times 21.3 \times 24 = N\ 511.20/\$1.25$$

Milling cost of the Starting materials (MCSM) = N 500.00k/$1.20

ChemistrySelect

Research Article
doi.org/10.1002/slct.202203816

Chemistry Europe
European Chemical
Societies Publishing

Calcination Cost of the Starting materials per unit loading (CCSM) = N (**h x u x c**)

Where "*h*" is the hour = 4 h, "*u*" is the unit loading and "*c*" is the cost per unit loading.

$$CCSM = 4 \times 1 \times N\ 250.00 = N\ 1000.00k/\$2.40$$

$$Net\ cost = CSM + WCSM + DCSM + MCSM + CCSM =$$
$$N\ (0.00 + 800 + 511.2 + 500 + 1000)$$
$$= N\ 4,011.20k/\$9.66$$

$$Overhead\ cost = 10\%\ of\ Net\ cost$$
$$= 0.1 \times 4,011.20 =$$
$$N\ 401.12k/\$0.97$$

$$Total\ cost = N\ 401.12/\$0.97 + N\ 4,011.20/\$9.66$$
$$= N\ 4,412.32/\$10.63$$

The cost of 500 g of potassium hydroxide (KOH) and sodium hydroxide (NaOH), the most used conventional homogeneous catalysts as of 14 January 2022, is N 7,000.00/\$16.55, respectively. This implies that 1000 g of these conventional catalysts will cost N14,000/\$33.10. Therefore, the cost used to produce 1000 g of each of the developed CPWSA, CMSHA and CLBPA, is 68.5% lower compared with the cost of conventional catalysts.

Conclusions

The study suggests a possible novel application of biogenic agricultural residues from periwinkle shells, melon seed husk, and locust bean pod husk, which were previously considered wastes. The following conclusions were made from the results obtained:

- The characterization of the calcined ash samples (CPWSA, CMSHA, and CLBPA) from these selected agricultural residues via EDS/EDX revealed variations of elements such as Na, K, Mg, Ca, Al, C, O, Mn, etc.
- The XRD revealed major diffraction peaks of CaO, Na_2O, K_2O and MgO crystalline phases at a calcination temperature of 800 °C in each catalyst, which further confirmed the presence of alkaline elements.
- The FTIR showed the presence of C=O, C–O, C–H, and O–H bonds as primary bonds in the catalysts.
- High basicity values of 11.65, 10.41, and 11.62 suggest the use of each catalyst as a potential heterogeneous catalyst.
- The CPWSA, CMSHA, and CLBPA were able to catalyze biodiesel production from PKO during catalyzed transesterification with ethanol.
- The CPWSA catalyst had the highest PKOEE yield of 84.38%.
- Except for the flash point and cetane number for the biodiesel samples obtained via the CMSHA and CLBPA catalyzed transesterification processes, all of the character-

istics were within the ASTM D6751 standard, and the fatty acid composition of the PKOEE is highly saturated.
- The production cost of each catalyst for 1000 g at different processing stages was N4,412.32/\$10.63, making them cost-effective.

From the results obtained, this research reveals possible innovative heterogeneous solid biobased catalysts that are cost-effective, ecologically favourable, and renewable, which may be utilized in catalytic amounts in biodiesel production. Further research should be conducted into the use of these catalysts (CPWSA, CMSHA, and CLBPA) as a composite heterogeneous base catalyst for the transesterification of oil into biodiesel.

Acknowledgements

Conflict of Interest

The authors declare no conflict of interest.

Data Availability Statement

The data that support the findings of this study are available from the corresponding author upon reasonable request.

[1] a) N. Sadia, N. Muhammad, Q. Liaqat Ali, A. Muhammad Shahbaz, S. Ali, A. Syed Danial, in *Biofuels* (Ed.: B. Krzysztof), IntechOpen, Rijeka, **2018**. Ch. 6; b) S. Dutta, K. K. Jaiswal, R. Verma, D. M. Basavaraju, A. P. Ramaswamy, *Biocatalysis and Agricultural Biotechnology* **2019**, *22*, 101390.

[2] a) B. Oladipo, E. Betiku, *J. Environ. Manage.* **2020**, *268*, 110705; b) S. Imtenan, M. Varman, H. H. Masjuki, M. A. Kalam, H. Sajjad, M. I. Arbab, I. M. R. Fattah, *Energy Convers. Manage.* **2014**, *80*, 329–356.

[3] E. Betiku, A. O. Etim, O. Pereao, T. V. Ojumu, *Energy Fuels* **2017**, *31*, 6182–6193.

[4] J. M. Rubio-Caballero, J. Santamaría-González, J. Mérida-Robles, R. Moreno-Tost, M. L. Alonso-Castillo, E. Vereda-Alonso, A. Jiménez-López, P. Maireles-Torres, *Fuel* **2013**, *105*, 518–522.

[5] a) J. A. Bennett, K. Wilson, A. F. Lee, *J. Mater. Chem. A* **2016**, *4*, 3617–3637; b) I. M. R. Fattah, H. H. Masjuki, M. A. Kalam, M. A. Hazrat, B. M. Masum, S. Imtenan, A. M. Ashraful, *Renewable Sustainable Energy Rev.* **2014**, *30*, 356–370.

[6] a) O. J. Alamu, M. A. Waheed, S. O. Jekayinfa, *Energy Sources, Part A: Recovery, Utilization, and Environmental Effects* **2009**, *31*, 1105–1114; b) O. Ogunkunle, O. O. Oniya, A. O. Adebayo, *Energy and Policy Research* **2017**, *4*, 21–28; c) C. E. Akhabue, O. S. Okwundu, *Biofuels* **2019**, *10*, 729–736.

[7] I. M. R. Fattah, H. C. Ong, T. M. I. Mahlia, M. Mofijur, A. S. Silitonga, S. M. A. Rahman, A. Ahmad, *Front. Energy Res.* **2020**, *8*.

[8] W. Xie, L. Zhao, *Energy Convers. Manage.* **2014**, *79*, 34–42.

ChemistrySelect

Research Article
doi.org/10.1002/slct.202203816

Chemistry Europe
European Chemical
Societies Publishing

[9] K. Ramachandran, P. Sivakumar, T. Suganya, S. Renganathan, *Bioresour. Technol.* **2011**, *102*, 7289–7293.

[10] W. Suryaputra, I. Winata, N. Indraswati, S. Ismadji, *Renewable Energy* **2013**, *50*, 795–799.

[11] a) M. Mofijur, H. H. Masjuki, M. A. Kalam, A. E. Atabani, I. M. R. Fattah, H. M. Mobarak, *Ind. Crops Prod.* **2014**, *53*, 78–84; b) M. F. M. A. Zamri, J. Milano, A. H. Shamsuddin, M. E. M. Roslan, S. F. Salleh, A. A. Rahman, R. Bahru, I. M. R. Fattah, T. M. I. Mahlia, *WIREs Energy and Environment* **2022**, */a*, e437.

[12] O. A. Falowo, B. Oladipo, A. E. Taiwo, T. A. Olaiya, O. Oyekola, E. Betiku, Research Square, **2021**.

[13] a) A. A. Akinola, B. Ayedun, M. Abubakar, M. Sheu, T. Abdoulaye, *Journal of Development and Agricultural Economics* **2015**, *7*, 162–173; b) S. O. Jekayinfa, J. I. Orisaleye, R. Pecenka, *Resources* **2020**, *9*, 92; c) X. Yin, X. Duan, Q. You, C. Dai, Z. Tan, X. Zhu, *Energy Convers. Manage.* **2016**, *112*, 199–207.

[14] N. Mansir, Y. H. Taufiq-Yap, U. Rashid, I. M. Lokman, *Energy Convers. Manage.* **2017**, *141*, 171–182.

[15] S. E. Onoji, S. E. Iyuke, A. I. Igbafe, M. O. Daramola, *Energy Fuels* **2017**, *31*, 6109–6119.

[16] Y. H. Tan, M. O. Abdullah, C. Nolasco-Hipolito, *Renewable Sustainable Energy Rev.* **2015**, *47*, 589–603.

[17] E. Betiku, A. M. Akintunde, T. V. Ojumu, *Energy* **2016**, *103*, 797–806.

[18] A. O. Etim, E. Betiku, S. O. Ajala, P. J. Olaniyi, T. V. Ojumu, *Sustainability* **2018**, *10*, 707.

[19] B. Nath, B. Das, P. Kalita, S. Basumatary, *J. Cleaner Prod.* **2019**, *239*, 118112.

[20] J. L. Aleman-Ramirez, J. Moreira, S. Torres-Arellano, A. Longoria, P. U. Okoye, P. J. Sebastian, *Fuel* **2021**, *284*, 118983.

[21] a) F. A. Olutoge, O. M. Okeyinka, O. S. Olaniyan, *International Journal of Research and Reviews in Applied Sciences* **2012**, *10*, 428–434; b) C. Okoye, C. Okey-Onyesolu, I. Nwokedi, O. Eije, E. Asimobi, *Journal of Energy Research and Reviews* **2020**, *4*, 32–43.

[22] B. Nyakuma, O. Oladokun, Y. Dodo, S. Wong, H. Uthman, M. Halim, *Chemistry & Chemical Technology* **2016**, *10*, 493–497.

[23] O. O. Olubajo, A. Jibril, O. A. Osha, *Path of Science* **2020**, *6*, 4001–4016.

[24] I. M. Mendonça, O. A. R. L. Paes, P. J. S. Maia, M. P. Souza, R. A. Almeida, C. C. Silva, S. Duvoisin, F. A. de Freitas, *Renewable Energy* **2019**, *130*, 103–110.

[25] P. U. Okoye, S. Wang, L. Xu, S. Li, J. Wang, L. Zhang, *Energy Convers. Manage.* **2019**, *179*, 192–200.

[26] A. Aladetuyi, G. A. Olatunji, D. S. Ogunniyi, T. E. Odetoye, S. O. Oguntoye, *Biofuel Research Journal* **2014**, *1*, 134–138.

[27] O. A. Falowo, T. V. Ojumu, O. Pereao, E. Betiku, *Catalysts* **2020**, *10*, 190.

[28] A. O. Etim, P. Musonge, A. C. Eloka-Eboka, *Biofuels, Bioproducts and Biorefining* **2020**, *14*, 620–649.

[29] S. H. Dhawane, T. Kumar, G. Halder, *Renewable Energy* **2016**, *89*, 506–514.

[30] V. O. Odude, A. J. Adesina, O. O. Oyetunde, O. O. Adeyemi, N. B. Ishola, A. O. Etim, E. Betiku, *Waste and Biomass Valorization* **2019**, *10*, 877–888.

[31] E. A. Olatundun, O. O. Borokini, E. Betiku, *Renewable Energy* **2020**, *166*, 163–175.

[32] Y. Kamikawa, J. Nishinaga, S. Ishizuka, T. Tayagaki, H. Guthrey, H. Shibata, K. Matsubara, S. Niki, *J. Appl. Phys.* **2018**, *123*, 093101.

[33] T. M. Shanahan, J. S. Pigati, D. L. Dettman, J. Quade, *Geochim. Cosmochim. Acta* **2005**, *69*, 3949–3966.

[34] S. Boonyuen, S. M. Smith, M. Malaithong, A. Prokaew, B. Cherdhirunkorn, A. Luengnaruemitchai, *J. Cleaner Prod.* **2018**, *177*, 925–929.

[35] J. L. Wray, F. Daniels, *J. Am. Chem. Soc.* **1957**, *79*, 2031–2034.

[36] M. O. Ekeoma, P. A. C. Okoye, V. I. E. Ajiwe, B. H. Hamed, *Journal of Chemical Society of Nigeria* **2016**, *41*, 130–136.

[37] J. Wang, L. Yang, W. Luo, G. Yang, C. Miao, J. Fu, S. Xing, P. Fan, P. Lv, Z. Wang, *Fuel* **2017**, *196*, 306–313.

[38] G. Pathak, D. Das, K. Rajkumari, S. L. Rokhum, *Green Chem.* **2018**, *20*, 2365–2373.

[39] E. Betiku, A. A. Okeleye, N. B. Ishola, A. S. Osunleke, T. V. Ojumu, *Catal. Lett.* **2019**, *149*, 1772–1787.

[40] G. G. Muciño, R. Romero, A. Ramírez, S. L. Martínez, R. Baeza-Jiménez, R. Natividad, *Fuel* **2014**, *138*, 143–148.

[41] T. D. Akpenpuun, B. A. Akinyemi, O. Olawale, O. J. Aladegboye, O. I. Adesina, *Journal of Applied Sciences and Environmental Management* **2019**, *23*, 377–382.

[42] C.-L. Lee, C.-C. Chang, H.-W. Kuo, W. Cheng, *Fish Shellfish Immunol.* **2020**, *107*, 357–366.

[43] M. Gohain, K. Laskar, H. Phukon, U. Bora, D. Kalita, D. Deka, *Waste Management* **2020**, *102*, 212–221.

[44] M. Balajii, S. Niju, *Energy Convers. Manage.* **2019**, *189*, 118–131.

[45] C. T. Oloyede, S. O. Jekayinfa, A. O. Alade, O. Oyetola, N.-A. U. Otung, O. T. Laseinde, *Engineering Reports*, n/a, e12585.

[46] C. E. Akhabue, J. A. Ogogo, *Ife Journal of Science* **2018**, *20*.

[47] O. J. Alamu, M. A. Waheed, S. O. Jekayinfa, *Energy for Sustainable Development* **2007**, *11*, 77–82.

[48] O. A. Falowo, B. Oladipo, A. E. Taiwo, A. T. Olaiya, O. O. Oyekola, E. Betiku, *Chemical Engineering Journal Advances* **2022**, *10*, 100293.

[49] S. A. Shahir, H. H. Masjuki, M. A. Kalam, A. Imran, S. I. M. R. Fattah, A. Sanjid, *Renewable Sustainable Energy Rev.* **2014**, *32*, 379–395.